Asian Journal of Chemistry; Vol. 30, No. 8 (2018), 1868-1872

ASIAN JOURNAL OF CHEMISTRY

https://doi.org/10.14233/ajchem.2018.21354

Enhanced Photocatalytic Activity of Visible Light Driven $Zr_{0.15}Mn_{0.85}Fe_2O_4$ Catalyst for Degradation of Organic Pollutant

A. ABILARASU[1], T. SOMANATHAN[1,*] and A. GEETHA BHAVANI[2]

[1]Department of Chemistry, School of Basic Sciences, Vels Institute of Science, Technology and Advanced Studies (VISTAS), Chennai-600 117, India
[2]Department of Chemistry, School of Sciences, Noida International University, Noida-203 201, India

*Corresponding author: Fax: +91 44 22662513; Tel: +91 44 22662500; E-mail: soma_nano@yahoo.co.in

Received: 28 March 2018; *Accepted*: 16 May 2018; *Published online*: 30 June 2018; AJC-18988

Zirconium incorporated manganese ferrite ($Zr_{0.15}Mn_{0.85}Fe_2O_4$) nanoparticles were prepared successfully by a solution combustion technique using glycine as a fuel. The samples were characterized using X-ray diffraction analysis and scanning electron microscopy. The XRD analysis confirmed the formation of spinel structure of the synthesized material. The photocatalytic activity of $Zr_{0.15}Mn_{0.85}Fe_2O_4$ nanoparticles has been examined for the photocatalytic degradation of direct blue 71 dye under visible light irradiation. It was found that the photocatalytic degradation efficiency of the catalyst increased with co-doping of zirconium. The reason for the enhanced photocatalytic activity of $Zr_{0.15}Mn_{0.85}Fe_2O_4$ mainly due to increased optical absorption and decreased recombination of electrons-holes. Hence present study also shows that $Zr_{0.15}Mn_{0.85}Fe_2O_4$ catalyst could be utilized as potential catalyst for the degradation of hazardous pollution and can be recovered from the reaction mixture using an external magnet and recycled.

Keywords: Manganese ferrite, Photo catalyst, Combustion technique, Visible light irradiation, X-Ray diffraction.

INTRODUCTION

Presently human facing big threat is water contamination due to over population, industrialization and improper wastewater management. Hazardous dyes are main pollutants discharged from the dying and other industries [1,2]. Industry effluent containing many hazardous organic pollutant, which are more stable so it doesn't remove by conventional wastewater treatment methods like precipitation, flocculation, ion-exchange, photodegradation, chemical oxidation and even microbiological treatment [3,4]. Advanced oxidation process (AOP) is powerful technique to degrade the pollutant from wastewater [5]. In modern days, magnetic catalysts are preferred to remove the pollutant from industries effluent. These types of magnetic photocatalyst are easily removed by external magnetic field from the system and it's reducing operational cost [6]. Recently spinel type ferrite nanomaterials widely used in many applications as storage, catalysis and environmental remediation because of high surface area, magnetic nature and chemical activity [7]. Manganese ferrite has been widely used for photocatalytic application due to high visible light response, good chemical stability and low cost [8]. To best of our knowledge no one report Zr doped manganese ferrite photocatalyst for the degradation of direct blue 71 under visible light irradiation. Therefore, we have synthesized $Zr_{0.15}Mn_{0.85}Fe_2O_4$ (ZMF) by solution combustion method and we study photocatalytic degradation efficiency of the catalyst for the degradation of direct blue 71 under visible light.

EXPERIMENTAL

Solution combustion method was used to synthesize the ferrite photocatalyst and the following metal nitrates such as manganese nitrate (Merck), ferric nitrate nonahydrate (Merck) and zirconium oxycholoride (Merck) are utilized as a metal precursors. In solution combustion synthesis fuel play a major role and glycine was utilized as a fuel.

Preparation of photocatalyst: We have synthesized the photocatalyst $Zr_{0.15}Mn_{0.85}Fe_2O_4$ (ZMF) according to reported method [9]. Zirconium doped manganese ferrite were synthesized by solution combustion method glycine used as fuel. Stoichiometric amount of ferric nitrate, manganese nitrate and zirconium oxychloride were prepared separately in millipore water. Thoroughly mix the precursor solution and add glycine. The mixed solution was kept in muffle furnace heated upto 550 °C for 5 min. The obtained catalyst was grounded into fine powder and used for further characterization. The synthesized catalyst characterized by high resolution scanning electron microscopy

(HRSEM) image AU_Quanta250FEG and X-ray diffraction (XRD) was carried out on G.E Inspection Technologies, XRD 3003 TT with CuK_α, $\lambda = 0.1541$ nm.

Photocatalytic degradation experiment: Catalytic degradation efficiency of the prepared material were examined by the photocatalytic degradation of direct blue 71 under visible light. All catalytic experiments were carried out at atmospheric conditions. The catalyst (20 mg) and direct blue 71 (30 mg/L) mixed solution was kept in dark room under stirring to attain adsorption-desorption equilibrium between direct blue 71 with the catalyst. Afterwards add H_2O_2 to the mixture and start illumination. During the experiment 5mL of sample were taken to calculate photocatalytic efficiency at given time interval. The disappearances of direct blue 71 was examined using Shimadzu UV-3600 Model at $\lambda_{max} = 594$ nm.

RESULTS AND DISCUSSION

XRD patterns: The synthesized material was examined by X-ray diffraction to determine the structural phase and crystalline nature of the photocatalyst are showed in Fig. 1. All diffraction peaks could be perfectly match with spinel cubic $MnFe_2O_4$ (JCPDS Card No. 73-1964). The X-ray diffraction peaks at 2θ of 18.39°, 30.59°, 35.72°, 43.34°, 53.62°, 57.04° and 62.56° correspond to the (111), (220), (311), (222), (400), (422), (511) and (440) planes, respectively [8,10,11]. The diffraction peaks at 33.40, 41.36, 51.35 and 54.53 can be indexed (002), (21-1), (122) and (221) planes of zirconium ion present in the synthesized materials [12].

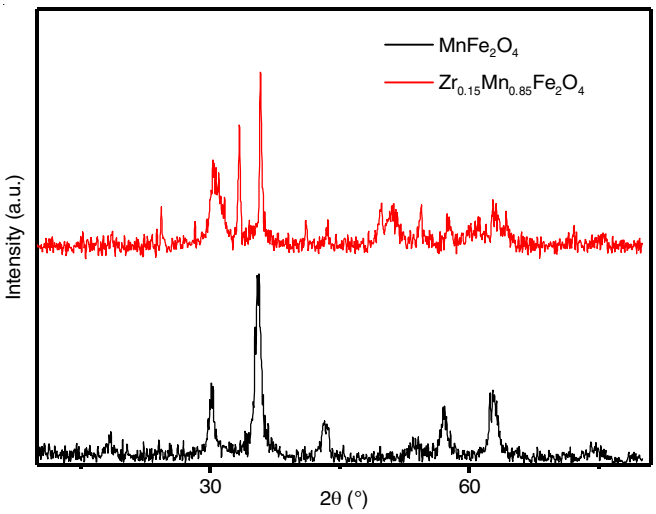

Fig. 1. XRD pattern of $MnFe_2O_4$ and $Zr_{0.15}Mn_{0.85}Fe_2O_4$

SEM analysis: The surface morphology of the synthesized sample was determined by scanning electron microscopy (SEM) and the images illustrated in Fig. 2. Based on HR-SEM analysis, the catalyst morphology appeared as irregular flakes like nanoparticles with agglomeration. The aggregation of the nanoparticle might be due to the presence of interfacial surface tension phenomenon [13]. Energy dispersive X-ray spectra of $Zr_{0.15}Mn_{0.85}Fe_2O_4$ are shown in Fig. 3. It confirms the presence of Zr, Fe, Mn and O elements. The observed atomic % of metal cations and anions are presented in Table-1.

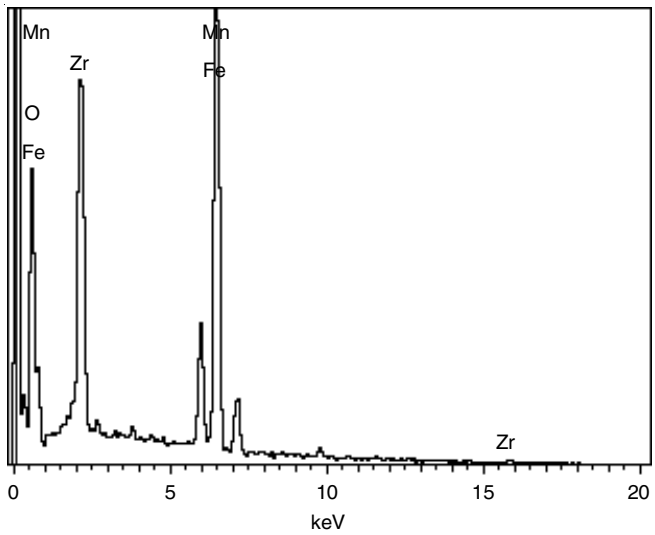

Fig. 3. EDX spectrum of ZMF

TABLE-1

Component	App. Conc.	Inten. Corrn	W (%)	W (%) Sigma	Atomic (%)
O K	29.61	0.9528	30.01	0.79	62.95
Mn K	9.18	0.9139	9.70	0.40	5.93
Fe K	37.26	0.9376	38.37	0.69	23.06
Zr K	16.91	0.7450	21.92	0.69	8.07

DRS-UV-visible spectral studies: Enhanced photocatalytic efficiency and photoinduced charge-transfer property of the photocatalyst are depending on their optical properties. UV-visible diffuse reflectance spectra (DRS) were used to examine the optical absorbance of synthesized material [14]. Fig. 4(a) shows the absorbance spectra of the catalyst. From the DRS UV spectra results we infer that the prepared samples strongly absorb both UV and visible region, which clearly confirms with previous study [15]. The band gap energy of

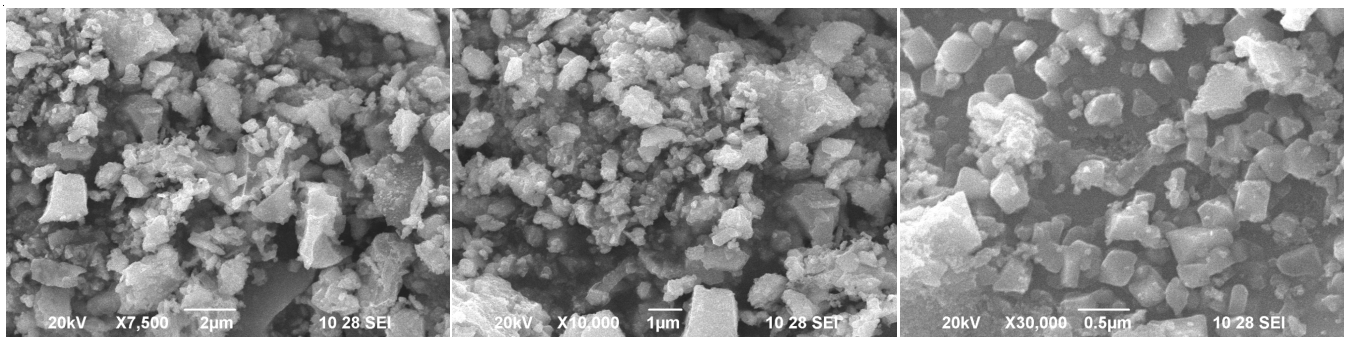

Fig. 2. SEM images of ferrite photocatalyst

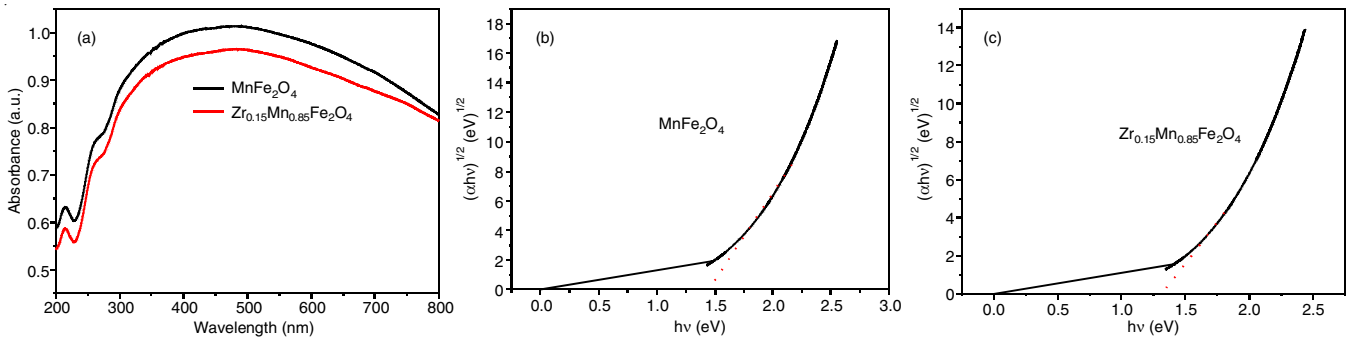

Fig. 4. (a) UV-visible DRS of the photocatalyst, (b) and (c) the corresponding band gap energy of $MnFe_2O_4$ and $Zr_{0.15}Mn_{0.85}Fe_2O_4$

pure $MnFe_2O_4$ and $Zr_{0.15}Mn_{0.85}Fe_2O_4$ is about 1.46 eV and 1.31 eV, respectively shown in Fig. 4(b) and 4(c). The results show that Zr doping decreases the band of the $MnFe_2O_4$ hence $Zr_{0.15}Mn_{0.85}Fe_2O_4$ has higher light absorption capability.

Photoluminescence spectroscopy: The photocatalytic activity of the catalyst is mainly depending on their charge separation and recombination of electron hole pairs. We estimate the rate of recombination process and charge separation by photoluminescence (PL) spectroscopy [16]. Photoluminescence emission spectra of the photocatalyst were recorded at an excitation wavelength of 280 nm and the result presented in Fig. 5. The emission peak appear around 540-650 nm is attributed to the emission of band gap transition, which was produced by the oxygen vacancy present on the surface of the catalyst. Photoluminescence intensity of the $Zr_{0.15}Mn_{0.85}Fe_2O_4$ is lower than pure $MnFe_2O_4$, which illustrate that Zr^+ ions effectively inhibit the rate of electron hole recombination. From the results we conclude that Zr^+ ions are responsible for the enhanced activity of the $Zr_{0.15}Mn_{0.85}Fe_2O_4$ photocatalyst [17].

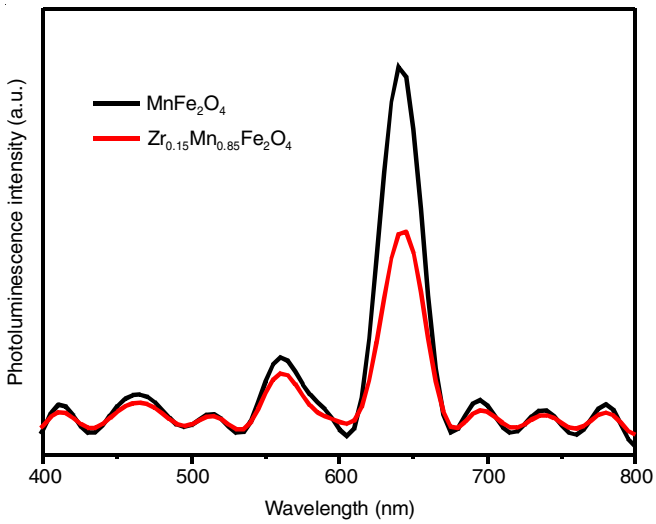

Fig. 5. Photoluminescence emission spectra of the photocatalyst

Catalytic activity of ferrite nanoparticle: In this study, synthesized nanomaterial used as a heterogeneous Fenton catalyst for the degradation of direct blue 71 in aqueous solution. We carried out two control reaction without addition of catalyst and H_2O_2 [18]. Photocatalytic degradation efficiency results of the catalyst are shown in Fig. 6. From the results we infer that the degradation of direct blue 71 almost negligible without catalyst and H_2O_2. Hence direct blue 71 very stable in

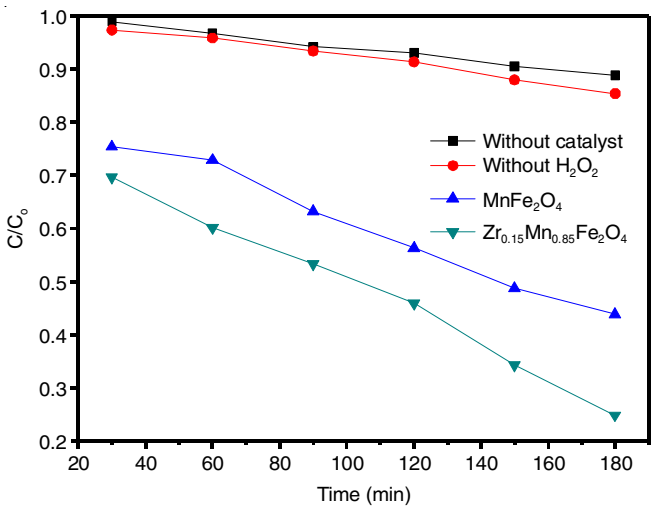

Fig. 6. Photocatalytic efficiency of the prepared samples

light irradiation in absence of H_2O_2 or catalyst. The degradation efficiency of $Zr_{0.15}Mn_{0.85}Fe_2O_4$ is high compare with pure manganese ferrite. The photo generated electrons are captured by zirconium it decline the recombination of electron-hole pair rate which enhance the degradation rate [19].

Effect of catalyst loading: Influence of the catalyst dosage has been evaluated to obtain optimum catalyst amount to remove the direct blue 71 in aqueous solution. Hence photocatalytic experiment carried out by varying the catalyst 0.2 to 0.8 g/L while other parameters remain constant and results shown in Fig. 7. Photocatalytic degradation efficiency increase with catalyst concentration increased 0.2 to 0.6 g/L because of relatively abundance of active sites on catalyst surface [20]. We increase catalyst amount beyond the optimum level photocatalytic degradation declined due to catalyst prevent light penetration into solution [21].

Influence of H_2O_2 concentration: Degradation rate of the Fenton process significantly depends on the concentration of H_2O_2. Fig. 8 illustrates the effect of H_2O_2 concentration on photocatalytic degradation efficiency. In order to evaluate obtain the optimum dosage of H_2O_2 amount [22]. The degradation rate enhanced with increase the amount of H_2O_2 due to more generation of hydroxyl radical. Beyond the optimum dosage considerable decrease in rate of the reaction could be attributed to the scavenging effect of hydroxyl radicals as follows. Hydroxyl radicals react with excess H_2O_2 to form hydroperoxyl radicals, which has lower potential to degrade the pollutant [23].

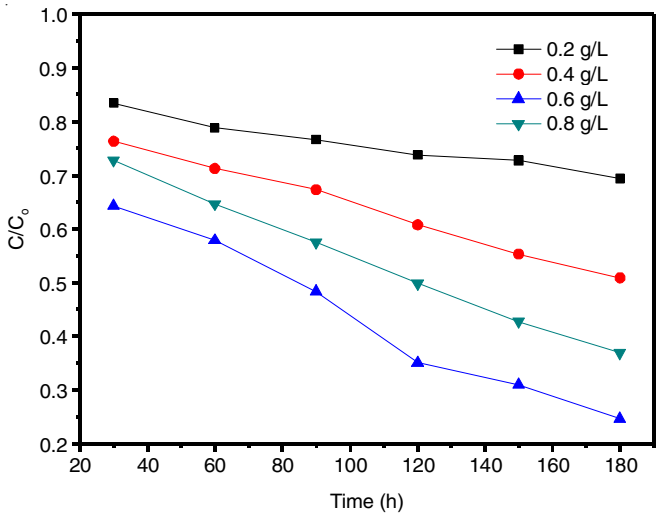

Fig. 7. Effect of catalyst amount

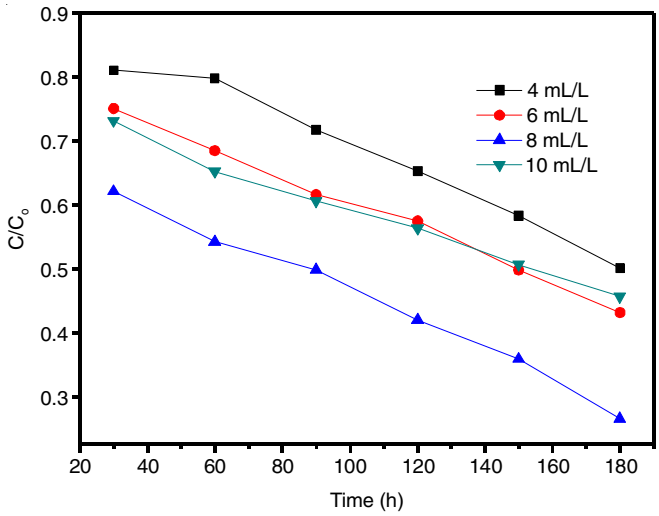

Fig. 8. Effect of H_2O_2 concentration

Reusability: Industrial point of view the recyclability of the photocatalyst is significant importance for practical application. Photocatalytic experiment carried to evaluate the reusability of the catalyst under visible light [24]. The result of the recyclability experiment is shown in Fig. 9. After the experiment

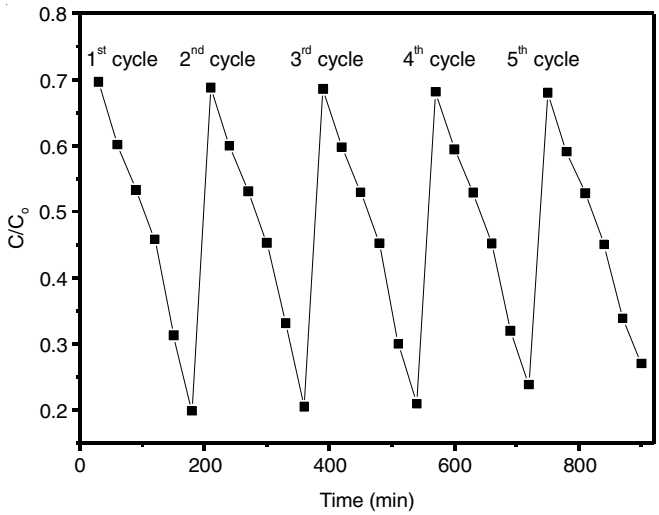

Fig. 9. Reusability of photocatalyst

catalyst removed using external magnet and washed several time with distilled water and dried. Degradation rate is decreased after 4th cycle is attributed to loss of catalyst during washing [25].

Conclusion

In summary, magnetic catalyst $Zr_{0.15}Mn_{0.85}Fe_2O_4$ were synthesized by facile, low cost, solution combustion method glycine as fuel. The prepared photocatalyst utilized as a hetrogenous Fenton catalyst for the degradation of direct blue 71 dye in presence of visible light. The enhancement of the degradation efficiency mainly attributed to the synergic effect of zirconium in spinel ferrite. It is concluded that the optimum condition to attain maximum efficiency is fixed as 0.6 g/L of photocatlyst and 8 mL/L of H_2O_2 concentration. The above mentioned catalyst can be recovered easily by external magnet and can be reused for the removal of hazardous pollutant from the wastewater.

ACKNOWLEDGEMENTS

One of the authors, T. Somanathan would like to thank the Department of Science and Technology (DST) for the award of Fast Track Young Scientist Award and also for providing financial support (SR/FT/CS-111/2011).

REFERENCES

1. P. Nuengmatcha, S. Chanthai, R. Mahachai and W. Oh, *J. Environ. Chem. Eng.*, **4**, 2170 (2016); https://doi.org/10.1016/j.jece.2016.03.045.
2. K. Kaviyarasu, E. Manikandan, J. Kennedy, M. Jayachandran, U.U. De Gomes, R. Ladchumananandasiivam and M. Maaza, *Ceram. Int.*, **42**, 8385 (2016); https://doi.org/10.1016/j.ceramint.2016.02.054.
3. Y. Yao, Y. Cai, F. Lu, F. Wei, X. Wang and S. Wang, *J. Hazard. Mater.*, **270**, 61 (2014); https://doi.org/10.1016/j.jhazmat.2014.01.027.
4. L. Yang, Y. Zhang, X. Liu, X. Jiang, Z. Zhang, T. Zhang and L. Zhang, *Chem. Eng. J.*, **246**, 88 (2014); https://doi.org/10.1016/j.cej.2014.02.044.
5. S. Yuan, Y. Fan, Y. Zhang, M. Tong and P. Liao, *Environ. Sci. Technol.*, **45**, 8514 (2011); https://doi.org/10.1021/es2022939.
6. N.M. Mahmoodi, *Desal. Water. Treat.*, **53**, 84 (2015); https://doi.org/10.1080/19443994.2013.834519.
7. Y. Du, W. Ma, P. Liu, B. Zou and J. Ma, *J. Hazard. Mater.*, **308**, 58 (2016); https://doi.org/10.1016/j.jhazmat.2016.01.035.
8. G. Mathubala, A. Manikandan, S. Arul Antony and P. Ramar, *J. Mol. Struct.*, **1113**, 79 (2016); https://doi.org/10.1016/j.molstruc.2016.02.032.
9. A. Abilarasu, A. Saravana and T. Somanathan, *J. Chem. Pharm. Sci.*, **4**, 111 (2014).
10. G.-Y. Yang, Y.-H. Ke, H.-F. Ren, C.-L. Liu, R.-Z. Yang and W.-S. Dong, *Chem. Eng. J.*, **283**, 759 (2016); https://doi.org/10.1016/j.cej.2015.08.027.
11. M.G. Naseri, E.B. Saion, H.A. Ahangar, M. Hashim and A.H. Shaari, *J. Magn. Magn. Mater.*, **323**, 1745 (2011); https://doi.org/10.1016/j.jmmm.2011.01.016.
12. M. Jafarpour, E. Rezapour, M. Ghahramaninezhad and A. Rezaeifard, *New J. Chem.*, **38**, 676 (2014); https://doi.org/10.1039/C3NJ00655G.
13. M. Sundararajan, L.J. Kennedy, P. Nithya, J.J. Vijaya and M. Bououdina, *J. Phys. Chem. Solids*, **108**, 61 (2017); https://doi.org/10.1016/j.jpcs.2017.04.002.
14. R. Jiang, H.-Y. Zhu, J.-B. Li, F.-Q. Fu, J. Yao, S.-T. Jiang and G.-M. Zeng, *Appl. Surf. Sci.*, **364**, 604 (2016); https://doi.org/10.1016/j.apsusc.2015.12.200.
15. M. Ge and Z. Hu, *Ceram. Int.*, **42**, 6510 (2016); https://doi.org/10.1016/j.ceramint.2016.01.035.

16. H.B. Jiang, J. Xing, Z.P. Chen, F. Tian, Q. Cuan, X.-Q. Gong and H.G. Yang, *Catal. Today*, **225**, 18 (2014); https://doi.org/10.1016/j.cattod.2013.08.027.
17. H. Zhu, M. Fang, Z. Huang, Y. Liu, K. Chen, C. Tang, M. Wang, L. Zhang and X. Wu, *RSC Adv.*, **6**, 56069 (2016); https://doi.org/10.1039/C6RA05098K.
18. M. Li, Q. Gao, T. Wang, Y.-S. Gong, B. Han, K.-S. Xia and C.-G. Zhou, *Mater. Des.*, **97**, 341 (2016); https://doi.org/10.1016/j.matdes.2016.02.103.
19. W. Chen, G.-R. Duan, T.-Y. Liu, Z.-M. Jia, X.-H. Liu, S.-M. Chen and X.-J. Yang, *J. Mater. Sci.*, **50**, 3920 (2015); https://doi.org/10.1007/s10853-015-8938-8.
20. R. Sharma, Komal, V. Kumar, S. Bansal and S. Singhal, *Mater. Res. Bull.*, **90**, 94 (2017); https://doi.org/10.1016/j.materresbull.2017.01.049.
21. R. Sharma, S. Bansal and S. Singhal, *RSC Adv.*, **5**, 6006 (2015); https://doi.org/10.1039/C4RA13692F.
22. T.D. Nguyen, N.H. Phan, M.H. Do and K.T. Ngo, *J. Hazard. Mater.*, **185**, 653 (2011); https://doi.org/10.1016/j.jhazmat.2010.09.068.
23. A. Flores, K. Nesprias, P. Vitale, J. Tasca, A. Lavat, N. Eyler and A. Cañizo, *Aust. J. Chem.*, **67**, 609 (2014); https://doi.org/10.1071/CH13435.
24. K. Vignesh, A. Suganthi, B.-K. Min and M. Kang, *J. Mol. Catal. A: Chem.*, **395**, 373 (2014); https://doi.org/10.1016/j.molcata.2014.08.040.
25. A. Manikandan, E. Hema, M. Durka, K. Seevakan, T. Alagesan and S. Arul Antony, *J. Supercond. Nov. Magnet.*, **28**, 1783 (2015); https://doi.org/10.1007/s10948-014-2945-x.